

# A Structural Investigation of T'-Pr<sub>2-x</sub>Ce<sub>x</sub>CuO<sub>4</sub> nanocrystals with $x = 0.13$

Putu Eka Dharma Putra,<sup>1,2</sup> I Gede Arjana,<sup>3</sup> Budi Hariyanto,<sup>4</sup> Resky Irfanita,<sup>5</sup> Malik Anjelh Baqiya\*,<sup>1</sup> and Darminto<sup>1</sup>

<sup>1</sup>Department of Physics, Institut Teknologi Sepuluh Nopember (ITS), ITS Campus, Keputih, Sukolilo, Surabaya 60111, Indonesia

<sup>2</sup>Institute of Materials and Optoelectronic Science, National Sun Yat-sen University (NSYSU) No. 70, Lienhai Rd., Kaohsiung 80424, Taiwan

<sup>3</sup>Department of Physics and Natural Science Education, Universitas Pendidikan Ganesha (Undiksha), Singaraja, Bali 81116, Indonesia

<sup>4</sup>Department of Physics, Universitas Palangka Raya (UPR), Kalimantan Tengah 73111, Indonesia

<sup>5</sup>Department of Physics, Faculty of Mathematics and Natural Science, Universitas Negeri Makassar, Jalan Daeng Tata Raya, Makassar 90223, Indonesia

**Abstract:** This report is briefly investigating the structural defect information of T'-Pr<sub>2-x</sub>Ce<sub>x</sub>CuO<sub>4</sub> (T'-PCCO) nanocrystals with  $x = 0.13$  at three different calcination temperatures. The as-synthesized powder of Pr<sub>2-x</sub>Ce<sub>x</sub>CuO<sub>4</sub> (PCCO) nanocrystals with  $x = 0.13$  were synthesized by using the chemically dissolved method within three different calcination temperatures, namely 900°C, 950°C, and 1000°C for 15 h in air. X-ray diffraction (XRD) technique is used to characterize the phase, structural, and crystalline defect information on the nanocrystal powder. It is found that all the indexed peaks are confirmed as PCCO phase with space group of I4/mmm and a minor impurity of Fm-3m space group. The lattice parameters are confirmed to be fluctuated signifying the stability of the Coulomb force at those temperatures. The post-Rietveld analysis using Bond Valance Sum (BVS) calculation shows the Ce-dependent of T'-PCCO nanocrystals while the Fourier difference suggests that the created crystalline defect as a part of the tetravalent doping effect which binds stronger apical oxygen. Moreover, at Pr- and Cu-site, the scattering distribution are fluctuating with the stable structure at 1000°C. This initial structural information is worth complementing the fundamental feature for understanding the T'-type cuprates.

Keywords: Apical oxygen; Bond valance sum (BVS); Crystalline defect; Fourier difference; T'-type structure

\*Corresponding author: amalikabits@physics.its.ac.id

Article history: Received 14 July 2021, Accepted 24 September 2021, Published October 2021.

<http://dx.doi.org/10.12962/j24604682.v17i3.9720>

2460-4682 ©Departemen Fisika, FSAD-ITS

## I. INTRODUCTION

The search of the high- $T_c$  superconductors (HTS) and their behavior opens a new hidden promising property. The so-called apical oxygen is known to be responsible for presenting magnetic behavior, namely, weak ferromagnetic features at room temperature [1]. By means the tetravalent ion doping, a crystalline defect may appear at the apical site and/or at the in-plane oxygen site exhibiting a dominant paramagnetic behavior with a minor weak ferromagnetic feature [2].

Since the beginning of the HTS development, the structural investigation on the magnetic properties is becoming the key role to unveil the fundamental feature of the superconducting materials. The so-called T'-type structure is one of the most emerging group of HTS that attracts many researchers around the world. The upturn resistivity of this type structure is associated to the existence of the apical oxygen [3] even at with or without rare earth ions doping referring to the strong electron correlated system [4]. Therefore, it needs a further attention at various point of view.

Among hundreds of HTS nanomaterials, the Pr<sub>2-x</sub>Ce<sub>x</sub>CuO<sub>4</sub> (PCCO) is one of the T'-type cuprates that has been extensively studied in the last two decades. The existence of the crystalline defect [2, 5], defect recovery

[6], and the local structure [7] on this T'-type structure has been well studied in gaining a fundamental understanding of the structural behavior at room temperature. The structural studies at the under doped regime [5] and upper doped regime [2, 8] of the T'-type cuprates have been explored in detail on the Ce-doping dependence in related to the crystalline defects due to annealing effect. Unfortunately, the detailed study of specific moderate tetravalent ionic doping has not been studied well. This later raise a question, how such a defect can appear and affect the origin feature of the structure.

Currently, it is found that the defect recovery on the T'-type structure can be strongly reduce the vacancy at the surface of the nanoparticles [6] in contrast to the full annealing oxygen reduction at vacuum atmosphere [1, 2]. This may be related to the number of vacancies recovered and/or created in the nanoparticles. Even so, the structural study on the weak ferromagnetic at room temperature may be routed out into its as-synthesized form at where the excess oxygen is created naturally. It is noted that the created crystalline defect may be differently presented as they are individually treated over various tetravalent ionic (electron type) doping. The electron type doping with specific calcination process may lead to a fundamental issue at where the moderate crystalline defect is formed to achieve the room temperature magnetism as well

mentioned in Ref. [2].

The focus now is pointed to the crystalline structure of the electron-doped cuprates, namely T'-PCCO nanocrystals with  $x = 0.13$  at different calcination temperatures. The tetravalent ionic doping of  $Ce^{4+}$  at specific  $x = 0.13$  into the parent compound of the T'-PCCO is noted as a boundary range of the underdoped regime that still exhibit a critical temperature ( $T_c$ ) and lying on the mixed region of antiferromagnetic (AFM) state and superconducting (SC) state [9]. By means investigate the structural analysis at various ranges of calcination temperature may solve the above issue and finally give a prior information about how the defect-associated structure at moderate Ce doping ( $x = 0.13$ ) level behaves.

## II. METHODS

The T'-PCCO nanocrystals with  $x = 0.13$  have been synthesized by using the so-called chemically dissolved method with  $HNO_3$  as a dissolved agent. The resulted crust-like precursor was then calcinated at three different temperatures, namely  $900^\circ C$ ,  $950^\circ C$ , and  $1000^\circ C$  for 15 h, respectively, in the air to produce the as-synthesized powder. All samples were characterized by using the X-ray diffraction (XRD) Philips X'Pert MPD, with a Cu  $K\alpha$  radiation  $1.5362 \text{ \AA}$  at room temperature. The phase information, *i.e.*, indexing and peak searching are firstly analysed by using Conograph software [10]. The resulted phase candidate was used as a starting point for the Rietveld analysis on the XRD data. The FullProf (FP)-suite [11] with the implemented Rietveld method is used to study the structural information, the scattering density distribution, including the bond valance sum (BVS) calculations to investigate the crystalline defect over all calcination temperatures.

## III. RESULTS AND DISCUSSION

The structural investigation is started by conducting the indexing analysis on the diffraction data. All the appeared peaks in every diffraction data are indexed as I4/mmm space group referring to PCCO phase with minor impurity of Fm-3m space group for  $PrO_2$  phase. In other words, the main phase on the sample is contributed by the parent phase of  $Pr_2CuO_4$  with 13% doping of Ce. The indexed XRD pattern for as-synthesized T'-PCCO powder with  $x = 0.13$  calcinated at  $900^\circ C$ ,  $950^\circ C$ , and  $1000^\circ C$  for 15 h is depicted in Fig. 1(a-c).

The detail indexing analysis of the samples is set as follows. The diffractometer parameters *i.e.*, wavelength and the zero-point shift used in this indexing are  $1.5362 \text{ \AA}$  and  $-0.004915^\circ$ , respectively. The zero-point shift is estimated from the reflection pair method [12] by using two peak positions that have a ratio of  $d$ -values equal to two-fold. Moreover, a set of sorting criteria is used to determine the best Bravais lattice and lattice constant. The main phase is seen through the de Wolff Figure of Merit ( $M$ ) because it gives preference to the lattice parameters with high symmetry, and has the best efficiency. Some other statistical parameters of the Figure of Merit are also considered due to the presence of the impurity peaks [13]. The

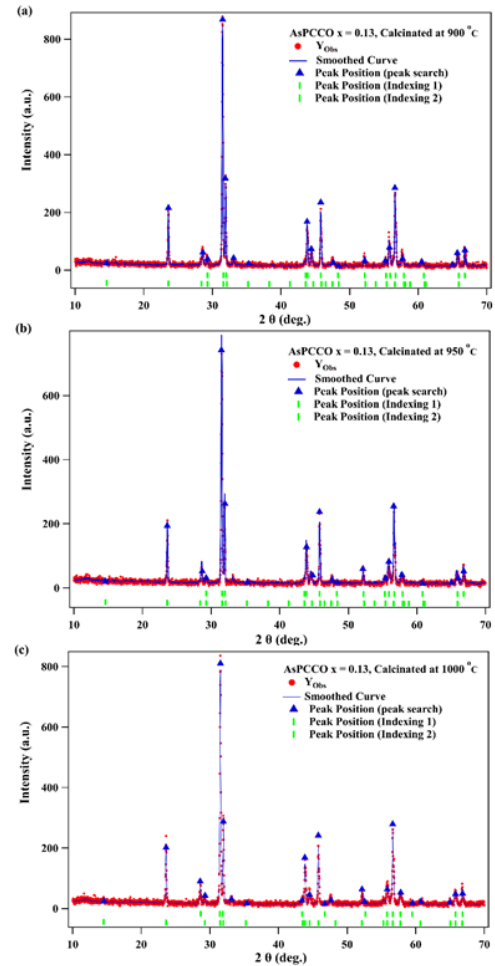


FIG. 1: Indexed XRD Profiles of as-synthesized T'-PCCO powders with  $x = 0.13$ , calcinated at (a)  $900^\circ C$ , (b)  $950^\circ C$ , (c)  $1000^\circ C$  for 15 h.

so-called Reverse Figure of Merit ( $M_{Rev}$ ) has been used due to its property which is opposite to that of the de Wolff Figure of Merit ( $M$ ). It is computed by exchanging the roles of observed peak positions and calculated peak positions in the definition of the de Wolff Figure of Merit ( $M$ ). This statistical figure of merit is sensitive to the existence of unobserved computed lines which is helpful to decide the presence of the impurity peaks. To satisfy the best decision, one can refer to the Ref. [10] in which  $M > 10$ ,  $M_{wll} > 10$ ,  $M_{Rev} > 3$ , or  $M_{Sym} > 30$  is in general likely to be the correct solution.

By using those considerations, it is found that all the samples possess the same Bravais lattice of Tetragonal (I) and Orthorhombic (F). Both the main phase of I4/mmm with  $M > 10$  and the minor phase of Fm-3m with  $M > 3$  are satisfied the sorting criteria. This emphasizes that all the samples have the same phase with a minor impurity even at different temperature range of the heat treatment. The complete results of this indexing are depicted in Table 1. The obtained lattice constant is used as the starting model in the refinement of the diffraction pattern.

Fig. 2 shows the refined XRD profile of the as-synthesized

TABLE I: Powder indexing and peaks searching of the As-synthesized T'-PCCO powder with  $x = 0.13$  at different calcination temperatures. Note: the de Wolff Figure of Merit ( $M$ ), Reverse Figure of Merit ( $M_{Rev}$ ), Wu Figure of Merit ( $M_{wu}$ ), and Symmetric Figure of Merit ( $M_{Sym}$ )

Calcination Temperature and Holding Time	Bravais Lattice Candidate	$M$ ; $M_{wu}$ ; $M_{Rev}$ ; $M_{Sym}$ ; $a, b, c$ [Å]; $\alpha, \beta, \gamma$ [deg.]
900°C, 15 h	Tetragonal (I)	<b>19.453</b> ; 6.370; 15.010; 121.550; 3.971, 3.971, 12.258; 90, 90, 90
	Orthorhombic (F)	4.180; 4.410; <b>8.031</b> ; 33.590; 5.595, 5.610, 12.156; 90, 90, 90
950°C, 15 h	Tetragonal (I)	<b>32.150</b> ; 11.036; 22.951; 297.22; 3.969, 3.969, 12.198; 90, 90, 90
	Orthorhombic (F)	5.200; 4.530; <b>3.100</b> ; 14.398; 5.100, 6.293, 12.198; 90, 90, 90
1000°C, 15 h	Tetragonal (I)	<b>65.960</b> ; 55.380; 2.740; 180.97; 3.968, 3.968, 12.231; 90, 90, 90
	Orthorhombic (F)	3.300; 2.680; <b>3.640</b> ; 11.743; 3.883, 5.600, 6.215; 90, 90, 90

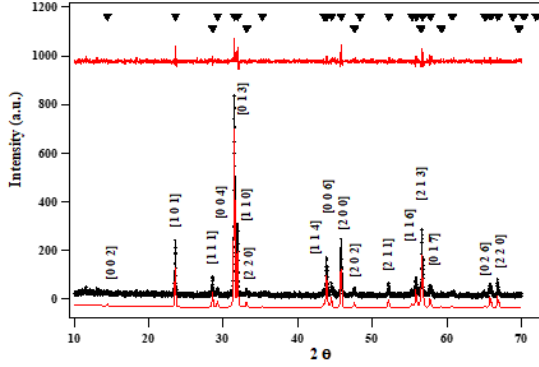


FIG. 2: Refined XRD Profiles of as-synthesized T'-PCCO powder with  $x = 0.13$  calcinated at 1000°C for 15 h.

T'-PCCO nanocrystals with  $x = 0.13$  calcinated at 1000°C for 15 h. All the presented peaks agree with the indexing result in Ref. [2]. A minor impurity of  $\text{PrO}_2$  is presented at a diffraction angle of 28.4° with (1 1 1) miller index and assumed to have no contribution to the whole properties of the crystals. Moreover, by employing the structure factor  $F_{hkl}$  calculation, all the Bragg reflections of the main phases of the three samples are found to have no systematical absences. This is due to the fact that all the refined (h k l) miller index from the sample reflection fit the reflection condition of  $h+k+l=2n$  resulting the non-zero structure factor.

The refined lattice parameter of the as-synthesized T'-PCCO nanocrystals with  $x = 0.13$ , are shown in Table 2. The main phase of the T'-PCCO and the negligible small impurity of  $\text{PrO}_2$  are well confirmed as previously done by the peak indexing analysis. The existence of the  $\text{PrO}_2$  may contribute to the formation of imperfect structures during the calcination process. As the comparison, the refined lattice parameters for the T'-PCC nanocrystals for  $x$  other than 0.13 [2] are not differ significantly to that indexing analysis in Table 1. The lattice parameter of  $c$ -axis length is fluctuated for the calcination temperature ranges indicating the temperature dependent of the stability of Coulomb interaction. In other words, the main phase of PCCO nanocrystals with the stable structure is expected to be formed at 1000°C for 15 h.

Furthermore, Table 2 also shows the statistical judgement of the Rietveld refinement for the T'-PCCO nanocrystals. In this report, the quality of the refinements is referred to the sorting criteria that has been used in the previous studies [2, 5] as well as in Ref. [14]. Unfortunately, the  $R$ -factor that mea-

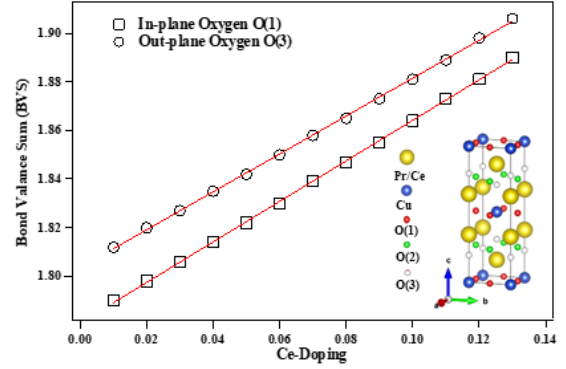


FIG. 3: The Bond Valence Sum Calculation for a range of Ce ( $x$ ) doping ( $x = 0.01$ -0.13) on the T'-PCCO Nano crystals.

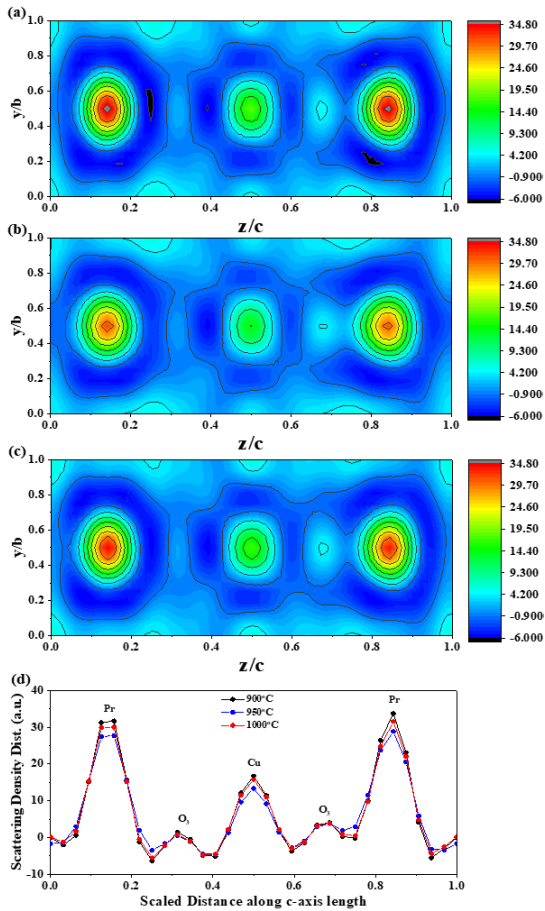
sures the agreement between the profiles intensity calculated from a crystallographic model and those obtained experimentally,  $R_p$ , including the weighted one,  $R_{wp}$ , are out of the sorting criteria. This may be compensated by the error measurement of the structure factor obtained from the T'-PCCO powder nanocrystals [15] and/or the wrong number of parameters included during the refinement process. Afterward, the statistical judgements are pointed into the goodness of fit ( $\chi^2$ ) together with the consideration of that error and the number of the refinement parameter included.

In order to estimate the effect of varying calcination temperature to the structural feature, namely, the bond valences of the different atoms, it is useful to calculate the values of bond valence sum (BVS). Fig. 3 shows the BVS calculation of the as-synthesized T'-PCCO nanocrystals with  $x = 0.13$ . In this calculation, the percentage of Ce doping concentration ( $x$ ) is varied ranging from 0% to 13% with a constraint to oxygen occupancy. This calculation reveals that the bond valence around the in-plane oxygen O(1) and the apical oxygen, O(3), respect to the center atom of Cu is Ce-dependent. The bond valence of these two oxygen sites increases linearly with  $x$  confirming stronger attraction to the Cu site. This may affect (i) a shrinking-down dimensional size of the  $c$ -axis length as reported in Ref. [2] and (ii) the ability to create vacancies at the  $\text{CuO}_2$  plane. In the underdoped regime, the bond-valence seems stronger rather than that in its parent compound [6]. This signifies that at a higher  $x$ , stronger energy must be compensated on the sample to create a vacancy.

Fig. 4(a-c) shows the Fourier difference map along the [0 y/b z/c] direction of the as-synthesized T'-PCCO with  $x =$

TABLE II: The refined lattice parameter of the as-synthesized T'-PCCO nanocrystals with  $x = 0.13$ 

PCCO Samples (Calcination Temperature and Holding Time)	Lattice Const. (Å)		$R_p$ (%)	$R_{wp}$ (%)	RB (%)	RF (%)	$\chi^2$ (%)	Frac. (%)
	a=b	c						
900°C, 15 h	$\text{Pr}_{1.87}\text{Ce}_{0.13}\text{CuO}_4$	3.958 12.218	30.1	31.2	9.05	8.13	1.54	95.10
	$\text{PrO}_2$	5.404 5.404						
950°C, 15 h	$\text{Pr}_{1.87}\text{Ce}_{0.13}\text{CuO}_4$	3.960 12.186	15.6	19.2	9.24	10.8	1.41	96.85
	$\text{PrO}_2$	5.402 5.402						
1000°C, 15 h	$\text{Pr}_{1.87}\text{Ce}_{0.13}\text{CuO}_4$	3.959 12.206	15.8	20.6	8.41	9.17	1.52	94.84
	$\text{PrO}_2$	5.402 5.401						

FIG. 4: Fourier Difference Map of the as-synthesized T'-PCCO with  $x = 0.13$ , calcinated at (a) 900°C, (b) 950°C, (c) 1000°C, and (d) the whole line profile with projection along  $c$ -axis length

0.13 calcinated at 900°C, 950°C, and 1000°C, respectively. It is found that the scattering density distribution at the Pr/Ce site is relatively fluctuated representing the crystalline and its defect stability at around the (Pr/Ce)-O plane and the apical oxygen site. Interestingly, the scattering density between these apical sites is likely not the same at the equivalence sites indicating an irregular scattering interaction related to their atomic vacancies. These can be also seen on the line profile of the same projection as depicted in Fig. 4(d). The scattering density distributions between Pr/Ce and Cu sites fluctuate

up to the calcination temperature of 1000°C while the scattering density distributions at the apical site shows no significant effect on those temperature variation. This indicates that the tetravalent doping into the Pr site yields a stronger bind on the apical oxygen to exhibit a complex small regular charge scattering. However, it is suggested to conduct a further check by using neutron diffraction rather than an x-ray diffraction technique due to the depth penetration issues.

#### IV. SUMMARY

The structural investigation of T'- $\text{Pr}_{2-x}\text{Ce}_x\text{CuO}_4$  (T'-PCCO) nanocrystals with  $x = 0.13$  at three different calcination temperatures has been successfully done. All the indexed peaks are confirmed as I4/mmm with minor impurity of Fm-3m space group referring to PCCO and  $\text{PrO}_2$  phase, respectively. The Rietveld analysis gives a clear picture of the fluctuated lattice parameter indicating the coulomb attraction stability at the given temperature range. The post-Rietveld analysis confirms the Ce-dependent of T'-PCCO nanocrystals which may affect the shrinking of crystalline volume and the ability to create a vacancy. A trace of tetravalent doping effect is found to bind the apical oxygen for higher  $x$ . Moreover, the scattering density distribution at around the Pr/Ce and Cu sites are relatively fluctuated in contrast to that at the O(3) site at the given temperature range. This indicates that the tetravalent doping into the Pr site yields a stronger binding on the apical oxygen to exhibit a complex small regular charge scattering distribution. This is reasonable since the thermal agitation from the calcination temperature is able to re-arrange the crystalline defect in the effect of Ce-doping. In other words, the variation of calcination temperatures has contribution to the presence of crystalline defect in the structure. This result provides a valid information of a stable calcination temperature for the T'-PCCO nanocrystals at the moderate tetravalent ionic doping.

#### Acknowledgment

This research was partly supported by the grant project Penelitian Dasar Unggulan Perguruan Tinggi Institut Teknologi Sepuluh Nopember (ITS) in the fiscal year of 2020-2021 from the Ministry of Research and Technology of the Republic of Indonesia (RISTEKBRIN).

- 
- [1] Baqiya MA, Putra PED, Irfanita R, *et al.*, "Enhanced Room- Temperature Ferromagnetism in Superconducting  $\text{Pr}_{2-x}\text{Ce}_x\text{CuO}_4$  Nanoparticles," *Materials Science Forum*, vol. 966, pp. 263268, 2019.
- [2] Baqiya MA, Putra PED, Triono B, *et al.*, "Ce-Doping and Reduction Annealing Effects on Magnetic Properties of  $\text{Pr}_{2-x}\text{Ce}_x\text{CuO}_4$  Nanoparticles," *Journal of Superconductivity and Novel Magnetism*, vol. 32, pp. 21652174, 2019.
- [3] Naito M, Krockenberger Y, Ikeda A, *et al.*, "Reassessment of the electronic state, magnetism, and superconductivity in high- $T_c$  cuprates with the  $\text{Nd}_2\text{CuO}_4$  structure," *Physica C: Superconductivity and its Applications*, vol. 523, pp. 2854, 2016.
- [4] Adachi T, Takahashi A, Suzuki KM, *et al.*, "Strong Electron Correlation behind the Superconductivity in Ce-Free and Ce-Underdoped high- $T_c$   $T'$ -Cuprates," *Journal of the Physical Society of Japan*, vol. 85, pp. 114716, 2016.
- [5] Putra PED, Irfanita R, Triono B, *et al.*, "Coexistence of weak ferromagnetism and paramagnetism in  $T'$ - $\text{Pr}_{2-x}\text{Ce}_x\text{CuO}_{4+\alpha-\delta}$  nanoparticles," *Key Engineering Materials*, vol. 855, pp. 134139, 2020.
- [6] Putra PED, Insani A, Irfanita R, *et al.*, "Possible Defect Recovery in  $T'$ - $\text{Pr}_{2-x}\text{Ce}_x\text{CuO}_4$  with  $x = 0.10$  Nanoparticles Analyzed by Neutron Diffraction," *Materials Science Forum*, vol. 1028, pp. 6874, 2021.
- [7] Irfanita R, Putra PED, Bambang T, *et al.*, "Oxygen Reduction Effect on  $T'$ - $\text{Pr}_{2-x}\text{Ce}_x\text{CuO}_4$  Nanopowders in the Underdoped Regime Studied by X-Ray Absorption Near Edge Structure," *Material Science Forum*, vol. 936, pp. 9397, 2018.
- [8] Irfanita R, Putra PED, Triono B, *et al.*, "Synchrotron X-Ray Absorption Spectroscopy (XAS) Studies on Structural and Magnetic Properties of  $T'$ - $\text{Pr}_{2-x}\text{Ce}_x\text{CuO}_4$  Nanocrystals," *Key Engineering Materials*, vol. 855, pp. 128133, 2020.
- [9] Armitage NP, Fournier P, Greene RL, "Progress and perspectives on electron-doped cuprates," *Reviews of Modern Physics*, vol. 82, pp. 24212487, 2010.
- [10] Esmaeili A, Kamiyama T, Oishi-Tomiyasu R, "New functions and graphical user interface attached to powder indexing software CONOGRAPH," *Journal of Applied Crystallography*, vol. 50, pp. 651659, 2017.
- [11] Rodriguez-Carvajal J, "Magnetic Structure Determination From Powder Diffraction Using The Program FullProf," in *Applied Crystallography. World Scientific*, pp. 3036.
- [12] Dong C, Wu F, Chen H, "Correction of zero shift in powder diffraction patterns using the reflection-pair method," *Journal of Applied Crystallography*, vol. 32, pp. 850853, 1999.
- [13] Oishi-Tomiyasu R, "Reversed de Wolff figure of merit and its application to powder indexing solutions," *Journal of Applied Crystallography*, vol. 46, pp. 12771282, 2013.
- [14] Kisi EH, "Rietveld analysis of powder diffraction patterns," *Materials Forum*, vol. 8, pp. 135155, 1994.
- [15] Wallwork SC, "Stephen C. Introduction to the calculation of structure factors", *International Union of Crystallography*, vol. 12, 1980.